metals

Article

Crystallization of Calcium Sulfate for Mining Wastewater Treatment

Fernanda Gusman Garreta Zamengo [1,*], Amilton Barbosa Botelho Junior [2], Marcelo Martins Seckler [1], Denise Crocce Romano Espinosa [1] and Jorge Alberto Soares Tenório [1]

[1] Department of Chemical Engineering, Polytechnic School, University of São Paulo (USP), São Paulo 05508-080, SP, Brazil; marcelo.seckler@usp.br (M.M.S.)
[2] Department of Materials Science and Engineering, Massachusetts Institute of Technology, Cambridge, MA 02139, USA; amilton.junior@alumni.usp.br
* Correspondence: fernandazamengo@usp.br

Abstract

This study aims to increase the particle size of the precipitate, aiming for an increasing settling speed. The effluent contains 21.88 g/L of sulfate, 526.5 mg/L of calcium, 2.9 mg/L of cadmium, 4.73 g/L of magnesium, 332.8 mg/L of manganese, and 205.8 mg/L of zinc. Based on thermodynamic simulations, evaluating the pH increase up to 9.0, it was possible to determine that the main species are $CaSO_4 \cdot 2H_2O$(s), $Mg(OH)_2$(s), MnO_2(s), ZnO(s), and $Cd(OH)_2$(s). In the precipitation tests, it was determined that a concentration of 2.0 mol/L of $Ca(OH)_2$ resulted in a particle size of 12.2 µm. The increase of temperature has an opposite effect, decreasing 40% of the particle size at 80 °C in comparison to 25 °C. On the other hand, the reaction time increases particle size, reaching 300% of an increase from 10 min to 3 h. In the seed tests, it was found that a seed ratio of 10 g/L to 100 g/L with the $CaSO_4$ (2) seed had the greatest impact on particle size growth, resulting in a 700% increase in particle size compared to the test without seeds. In the settling tests, a sedimentation rate of 177 mL/min was achieved using seeds and flocculants, compared to 50 mL/min in the test without reagents.

Keywords: seeds; settling; precipitation; nucleation

check for updates

Academic Editor: Jean François Blais

Received: 15 May 2025
Revised: 13 June 2025
Accepted: 18 June 2025
Published: 26 June 2025

Citation: Zamengo, F.G.G.; Botelho Junior, A.B.; Seckler, M.M.; Espinosa, D.C.R.; Tenório, J.A.S. Crystallization of Calcium Sulfate for Mining Wastewater Treatment. *Metals* **2025**, *15*, 710. https://doi.org/10.3390/met15070710

Copyright: © 2025 by the authors. Licensee MDPI, Basel, Switzerland. This article is an open access article distributed under the terms and conditions of the Creative Commons Attribution (CC BY) license (https://creativecommons.org/licenses/by/4.0/).

1. Introduction

Crystallization can be divided into four methods: cooling, evaporation, precipitation and anti-solvent crystallization. Cooling crystallization occurs through the decrease in the temperature, while evaporation occurs through the opposite. Precipitation occurs with the addition of a compound that reacts with the solute forming an insoluble compound, and anti-solvent crystallization happens with the addition of a solvent where the solute has a lower solubility [1].

The main force that guides crystallization is supersaturation (Δc, Equation (1), where c is the concentration and c* is the equilibrium concentration). The nucleation process occurs when supersaturation is achieved, and crystals are formed. Nucleation can be divided into primary and secondary categories, and primary crystallization can be divided into homogenous and heterogenous categories [2].

$$\Delta c = c - c^* \quad (1)$$

Primary nucleation happens in the absence of crystals, while secondary nucleation happens in the presence of crystals. A homogeneous primary nucleation occurs starting with the clear solution (e.g., without the presence of crystals), whilst the heterogeneous primary nucleation occurs in the presence of other substances (e.g., sodium chloride crystals in the crystallization of calcium sulfate) [1]. Secondary nucleation, on the other hand, occurs in the presence of crystals of the solute (also known as seeds). This technique can help control the characteristics of the crystals formed since the ions deposit around the seeds, instead of crystallizing on their own, that can help suppress the primary nucleation and support crystal growth [3].

Crystallization is applied in different industries, such as pharmaceutical and chemical industries, and has been successfully applied for wastewater treatment as a purification process [4]. Another application of crystallization is in mining for wastewater treatment. For instance, in 2023, 19.2 billion metric tons of minerals were mined, reflecting a generation of tons of wastewater containing residues and impurities that need further treatment [5].

Crystallization in wastewater with the presence of sulfates have been studied before, with authors Talebi, Rezaei and Rafiei [6] applying sodium carbonate and sodium sulfate to remove lithium and strontium from a solution. Another study focused on the recovery of manganese from mining wastewater using seeds [7]. Authors Yang et al. [8] studied the recovery of potassium and phosphorus from wastewater through the crystallization of magnesium potassium phosphate.

For the evaluation of crystallization in mining wastewater treatment, we studied the zinc mining wastewater provided by a zinc refinery located in Minas Gerais, Brazil, and it was a mixed effluent of different stages of the process including flotation and leaching.

In the current process, there is a stage for $Zn(OH)_2$ precipitation (Equation (2)) using $Ca(OH)_2$ at pH 7.0, and then after solid–liquid separation, more $Ca(OH)_2$ is added until reaching a pH of 9.0 for impurity removal. Our study focused on wastewater treatment after $Zn(OH)_2$ precipitation and aimed to improve the removal of impurities and $CaSO_4$.

$$ZnSO_4 + Ca(OH)_2 \rightarrow Zn(OH)_2 + CaSO_4 \quad (2)$$

The main gap in the current process is the decantation time that can take hours due to the small particle size distribution [9]. Depending on the supersaturation level, and the crystal particle sizes, the decantation process can take a higher time, leading to a less efficient process [10].

Therefore, the aim of this study was to increase the particle size of the precipitate formed in the second $Ca(OH)_2$ treatment. The method developed can be adapted for other industrial processes, allowing for increased efficiency in wastewater treatment, reducing operational costs, and with potential for upscaling. Our novel investigation is the evaluation and adjustment of precipitation parameters to promote controlled particle growth during the treatment of zinc mining effluent, with the aim of accelerating the decantation process and increasing the efficiency of the solid–liquid separation process.

2. Materials and Methods

2.1. Materials

The wastewater was characterized by an inductively coupled plasma optical emission spectrometer (ICP-OES) for the determination of Ca, Cd, Mg, Mn, and Zn using calibration curves of 0.1–1.0 mg/L and 1.0–10.0 mg/L in HNO_3 3%, and ion chromatography for the determination of sulfate with a calibration curve of 1.0–10.0 mg/L in ultrapure water.

The precipitating agent used was $Ca(OH)_2$. This reagent was prepared with the addition of the $Ca(OH)_2$ mass to ultrapure water. The mass was relative to the concentration

evaluated. The reagent was maintained in constant stirring to assure the homogeneity, given the low solubility of $Ca(OH)_2$ (0.17 g/100 mL of water at 20 °C) [11].

For the precipitation experiments, five seeds were evaluated. Two of the seeds were based on the methodology of Chagwedera, Chivavava, and Lewis (2022) [12]. These seeds were prepared with the addition of a 0.6 mol/L solution of $CaCl_2$ to a 0.6 mol/L solution of Na_2SO_4 at 70 °C and then filtered (0.45 µm). The crystals formed were washed four times with ultrapure water to remove the NaCl and analyzed. The seed labeled $CaSO_4$ (1) (Figure 1b) is this seed passed through a 25 µm sieve to have a more similar size to the other seeds evaluated, and the $CaSO_4$ (2) (Figure 1a) seed was the original size (39 µm). The other 3 types of seeds (Figure 1c) were recirculated from the process formed in the 10, 20, and 30 min experiments.

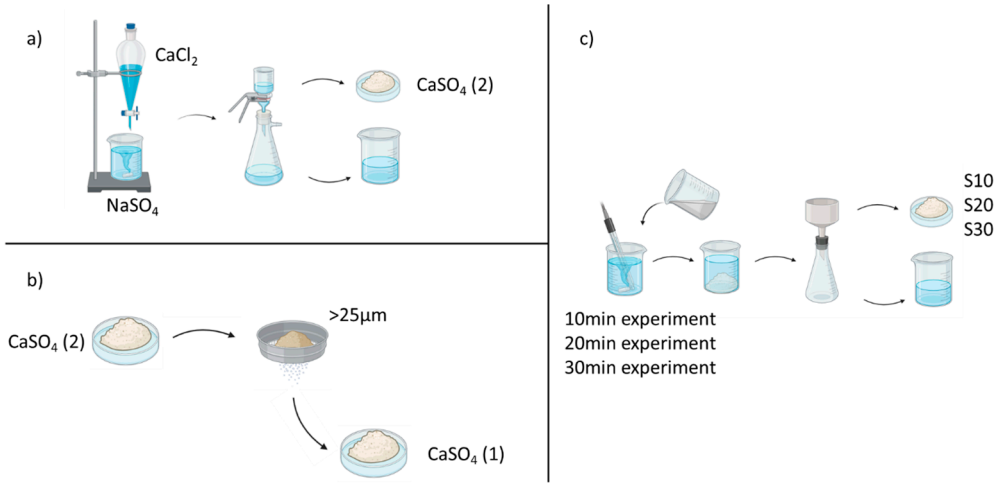

Figure 1. Diagram representing the different seeds' production, where two seeds were prepared from solution and sieving and three seeds were recirculated from the time experiments.

A synthetic solution was used for the decantation experiments given that 2 L were necessary per experiment and the sample received was insufficient. The synthetic solution was prepared with $CaCl_2$, $MgSO_4$, $ZnSO_4 \cdot 7H_2O$, $MnCl_2 \cdot 2H_2O$, $Cd(OH)_2 \cdot XH_2O$, and H_2SO_4 to simulate the concentrations of the real solution. The pH was adjusted to 7.0 with NH_4OH. This solution presented the same aspect of the sample when prepared.

2.2. Methods

2.2.1. Thermodynamic Simulations

Thermodynamic simulations were carried out for a better understanding of the solution behavior in our precipitation experiments. FactSage 8.3 was used to formulate Pourbaix diagrams and to determine the precipitation of the metals. Phreeqc Interactive 3.7.3 was used to perform a speciation calculation providing the species in solution and the degree of supersaturation. The limitations of the software are the databases, which should include the species studied. Phreeqc Interactive 3.7.3 is recommended when dealing with diluted solutions, such as the sample studied.

2.2.2. Precipitation Experiments

Precipitation experiments were carried out with 100 mL of solution in a beaker under magnetic stirring and constant pH measurement. A suspension of $Ca(OH)_2$ was added until the pH reached 9.0. Then, the solid–liquid mixture was filtered in a vacuum pump with a 2 µm filter, and the precipitate (solid) was washed using ultrapure water. The average particle size distribution was determined by SEM-EDS where the dried sample

was attached to the stub with a carbon tape and submitted to a vacuum chamber before analysis for unattached sample removal.

The effects of $Ca(OH)_2$ concentration (1.0 mol/L, 1.5 mol/L, and 2.0 mol/L), temperature (25 °C, 50 °C, 60 °C and 80 °C), and reaction time (10 min, 20 min, 30 min, 1 h, 2 h, and 3 h) were evaluated aiming to increase the particle size. These parameters can affect the nucleation of the crystals formed and therefore their impacts on the particle size were studied [1].

Another technique evaluated was seeding, where crystals were added in the solution prior to the $Ca(OH)_2$ suspension for better control of the precipitate characteristics and size [13]. Different seeds and proportions were analyzed, and a 2.0 mol/L $Ca(OH)_2$ suspension was later added until the pH reached 9.0 (25 °C for 1 h). The five seeds evaluated were tested in the proportion of 0.5 g/L. Following this, the seed with the higher particle size was evaluated with the proportions of 0.5, 1.0, 5.0, 10, and 50 (g/L), based on the levels defined by He et al. (2020) [3].

2.2.3. Decantation Experiments

Decantation experiments were carried out to verify the impact of the particle size in a 2 L graduated cylinder [14]. A precipitation experiment was carried out for 1 h at 25 °C with the addition of a suspension of $Ca(OH)_2$ at 2 mol/L until a pH of 9.0 was reached. The solid–liquid mixture was then added into the graduated cylinder and decantation time was measured. Four reagents evaluated were provided by Clariant S.A. and will be denominated as F1, F2, F3, and F4, and seeds were evaluated as well. Table 1 displays the reagents' characteristics as well as the proportion used in the decantation experiment by the company recommendation.

Table 1. Characteristics and proportions of the reagents evaluated.

Reagent (Commercial Name)	Characteristic	Proportion
F1 (Floticor AD17797)	Polymer coagulant	0.05% m/m
F2 (Floticor AD17097)	Polymer coagulant	0.05% m/m
F3 (Floticor AD18011)	Mineral coagulant	0.05% m/m
F4 (Floticor FL7130)	Anionic flocculant	0.01% m/m

The seeds were added prior to the suspension of $Ca(OH)_2$, as in the precipitation experiments, while the reagents were added soon after the 1 h had passed and this was maintained under low-medium stirring for 1 min, before being added to the graduated cylinder.

3. Results and Discussion

3.1. Solution Characterization and Thermodynamic Simulations

The chemical characterization of the tailing sample is displayed in Table 2. These concentrations can be expected due to the composition of the zinc ore used in the process (willemite) containing Ca, Cd, Mg, Mn, and Zn [15,16]. The SO_4^{2-} concentration is also expected, owing to the H_2SO_4 leaching process [17].

Table 2. Chemical characterization of the tailing sample in ICP-OES and IC.

SO_4^{2-}	Ca	Cd	Mg	Mn	Zn
21.8 g/L	526 mg/L	2.9 mg/L	4.7 g/L	332 mg/L	206 mg/L

Thermodynamic simulations were carried out to determine the species for each ion and to evaluate how the pH can influence precipitation. It was possible to determine the

species present in the solution, as well as concentration (Table 3) and the supersaturation of the compounds (Table 4).

Table 3. Concentration of the species/compounds in solution determined through Phreeqc Interactive 3.7.3.

Species/Compounds	Concentration (mg/L)
$CaSO_4$	947
Ca^{2+}	263
$Cd(SO_4)_2^{2-}$	3.7
$CdSO_4$	1.6
Cd^{2+}	0.7
$MgSO_4$	11,291
Mg^{2+}	2584
$MnSO_4$	452
Mn^{2+}	178
SO_4^{2-}	12,536
Zn^{2+}	206

Table 4. Supersaturation of the compounds determined through Phreeqc Interactive 3.7.3.

Compound	Supersaturation
$CaSO_4$	−0.03
$CaSO_4 \cdot 2H_2O$	0.14
CdO	−6.99
$Cd(OH)_2$	−5.75
MgO	−9.26
$Mg(OH)_2$	−4.78
MnO	−7.09
$Mn(OH)_2$	−4.49

This information was important to predict which compounds will precipitate in the process, while the supersaturation determines which compounds are on the verge of precipitating. If the supersaturation is positive, as it was for $CaSO_4 \cdot 2H_2O$ (0.14, Table 4), the compound will precipitate in the sample conditions, although the supersaturation is near 0, requiring a large amount of time to process.

Abdel-All, Rashad, and El-Shall (2004) [18] studied the supersaturation effect on the induction time in $CaSO_4$ crystallization, where a supersaturation of 1.301 resulted in the start of nucleation in 66.7 min, whilst a supersaturation of 1.880 resulted in the start of nucleation in 11.7 min. When comparing the authors' results with the supersaturation of the sample, it is possible to imply that a supersaturation of 0.14 (Table 4) is not adequate for precipitation in a practical amount of time, hence the addition of the suspension of $Ca(OH)_2$ to increase the Ca^{2+} concentration.

Pourbaix diagrams were prepared considering the sample conditions as received. The red dots on Figure 2 represent the sample conditions, and the green dots represent the conditions at a pH of 9.0. It is possible to determine that these five metals may precipitate as $CaSO_4$, $Mg(OH)_2$, ZnO, MnO, and $Cd(OH)_2$.

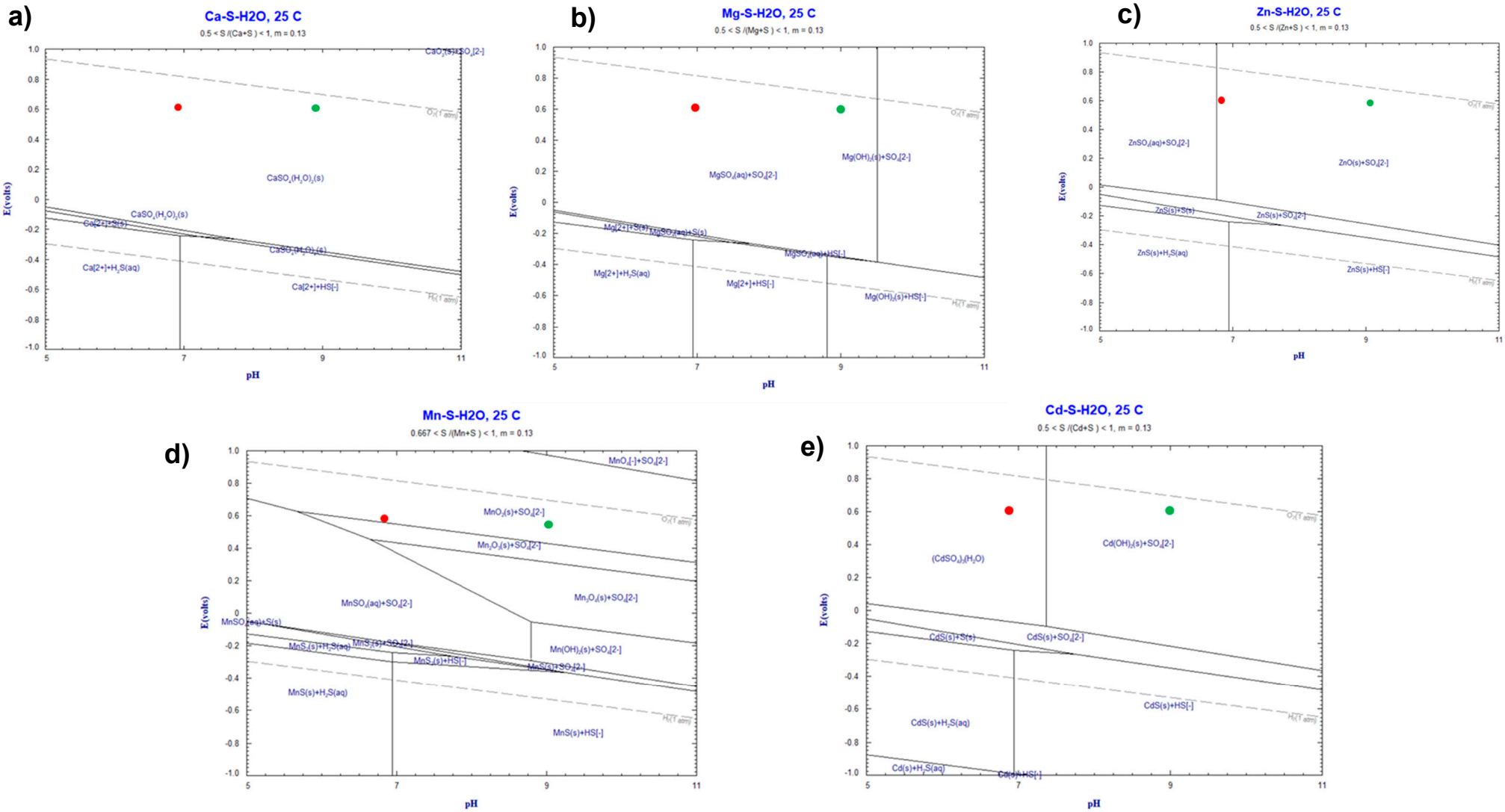

Figure 2. Diagrams of Eh/pH prepared in Factsage 8.3 for (**a**) Ca-S-H_2O, (**b**) Mg-S-H_2O, (**c**) Zn-S-H_2O, (**d**) Mn-S-H_2O, and (**e**) Cd-S-H_2O.

3.2. Precipitation Experiments Without Seeds

The effects of the concentration of the $Ca(OH)_2$ suspension, temperature, and time on the particle size were evaluated. Particle size increased with the increase in the $Ca(OH)_2$ concentration suspension (Figure 3a) because of solution supersaturation, as there is a predominance of the growth of the already-formed particles over the formation of new particles, which can be explained by the crystal growth equation ($G_N = k_{g,s}\sigma^g f(L)$) which shows a direct dependence between the crystal growth (G_N) and the supersaturation (σ) [2]. We also made thermodynamic simulations in Phreeqc Interactive 3.7.3 with the addition of $Ca(OH)_2$ in different concentrations to the sample, which resulted in a $CaSO_4{\cdot}2H_2O$ supersaturation of 0.95 for 1.0 mol/L, 1.07 for 1.5 mol/L, and 1.15 for 2.0 mol/L. The mean particle size was 7.1 µm at 1.0 mol/L, 7.1 µm at 1.5 mol/L, and 12.3 µm at 2.0 mol/L.

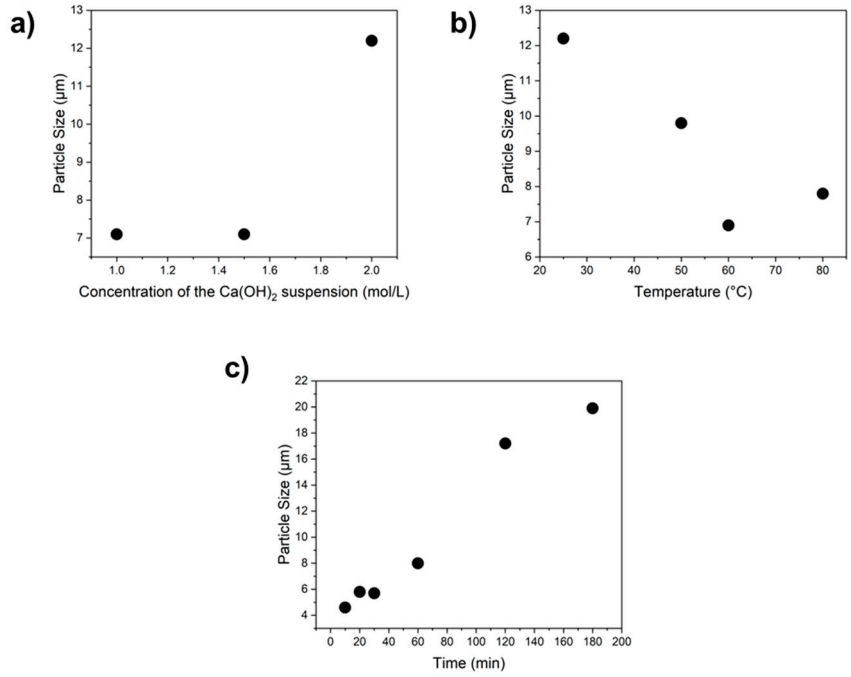

Figure 3. The effect of the concentration of $Ca(OH)_2$ suspension (**a**), temperature (**b**), and time (**c**) on the particle size.

The temperature causes the opposite effect and decreases the particle size as $CaSO_4$ solubility decreases with the increase in temperature; at 20 °C, the solubility is 3.0 g/L and at 80 °C, it is around 1.0 g/L [19]. Therefore, the degree of supersaturation increases rapidly, leading to primary nucleation, where smaller nucleus are formed rather than the growth of the crystal already formed. The equation that correlates the size of the critical nucleus formed (r*) with the temperature (T) also shows an inverse relationship ($r* = \frac{2\sigma}{p_s|\Delta\mu|}$ where $\Delta\mu = -k\ T\ lnS$); the equation also presents that the nucleus is dependent on the surface interface (σ) and the density of the nucleus formed (p_s) [20]. The mean particle size at 25 °C was 12.3 µm, at 50 °C was 9.8 µm, at 60 °C was 7.0 µm, and at 80 °C was 7.8 µm (Figure 3b). This effect was also observed by Luo et al. (2010) [21] when studying the influence of temperature on the morphology and structure of calcium sulfate, where the increase in temperature from 20 °C to 100 °C led to a decrease in particle size.

The increase in reaction time also increased the particle size due to supersaturation decrease over time and also the Ostwald ripening, where the smaller particles tend to dissolve and the ions re-deposit onto larger particles [22]. The equation that guides the Ostwald ripening ($r*(t) = r_0 * \left(\frac{t}{\tau_D^J}\right)^{1/2}$) demonstrates a direct dependence between the particle size (r*(t)) and the time (t) [23]. The mean particle size at 10 min was 4.6 µm, at

20 min was 5.8 µm, at 30 min was 5.7 µm, at 60 min was 8.0 µm, at 120 min was 17.3 µm, and at 180 min was 20.0 µm (Figure 3c). In crystallization without seeds, the ions in solution gather in a cluster forming a nucleus that dissolves and recrystallizes continuously, until a critical size is reached and this nucleus grows into a crystal over time (Figure 4).

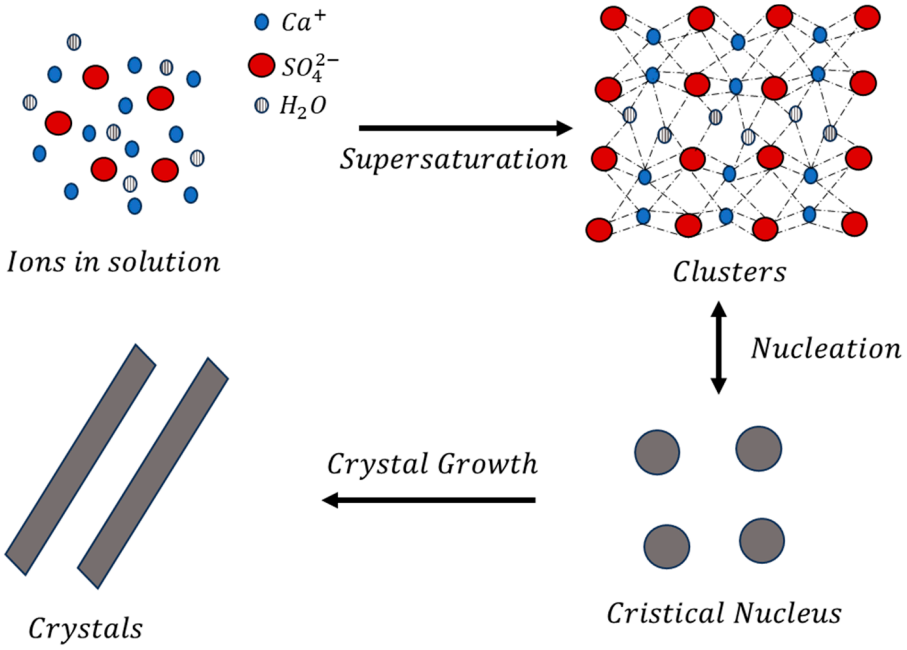

Figure 4. Diagram representing the crystallization phenomena.

When comparing the experiments without seeds, needle-like-shaped crystals are formed, typically with the $CaSO_4$ morphology (Figure 5a,b,e,f), with the increase in concentration and time. The rising of the temperature (Figure 5c,d) also demonstrated an aggregation of the particles formed, although they had a smaller size compared to the other conditions.

3.3. Precipitation Experiments with Seeds

The use of seeds in crystallization promotes secondary nucleation, increasing the particle size distribution. We evaluated five types of seeds and different proportions. The seeds labeled S10, S20, and S30 were recirculated from the precipitation process at 10 min, 20 min, and 30 min, and the labeled $CaSO_4$ (1) and (2) were based on the work of Chagwedera, Chivavava, Lewis (2022) [12]. Table 5 presents the seeds' mean particle size and the particle size achieved in the experiment. All experiments had the following conditions: 1 h, 25 °C, 2.0 mol/L of $Ca(OH)_2$ to elevate the pH until it reached 9.0, and a seed proportion of 0.5 g/L.

Table 5. Seed mean size and particle size achieved with seeded experiments.

Seed	Seed Mean Size	Particle Size Achieved
S10	4.6 µm	8.5 µm
S20	5.8 µm	9.0 µm
S30	5.7 µm	8.0 µm
$CaSO_4$ (1)	5.6 µm	23.4 µm
$CaSO_4$ (2)	39.0 µm	40.8 µm

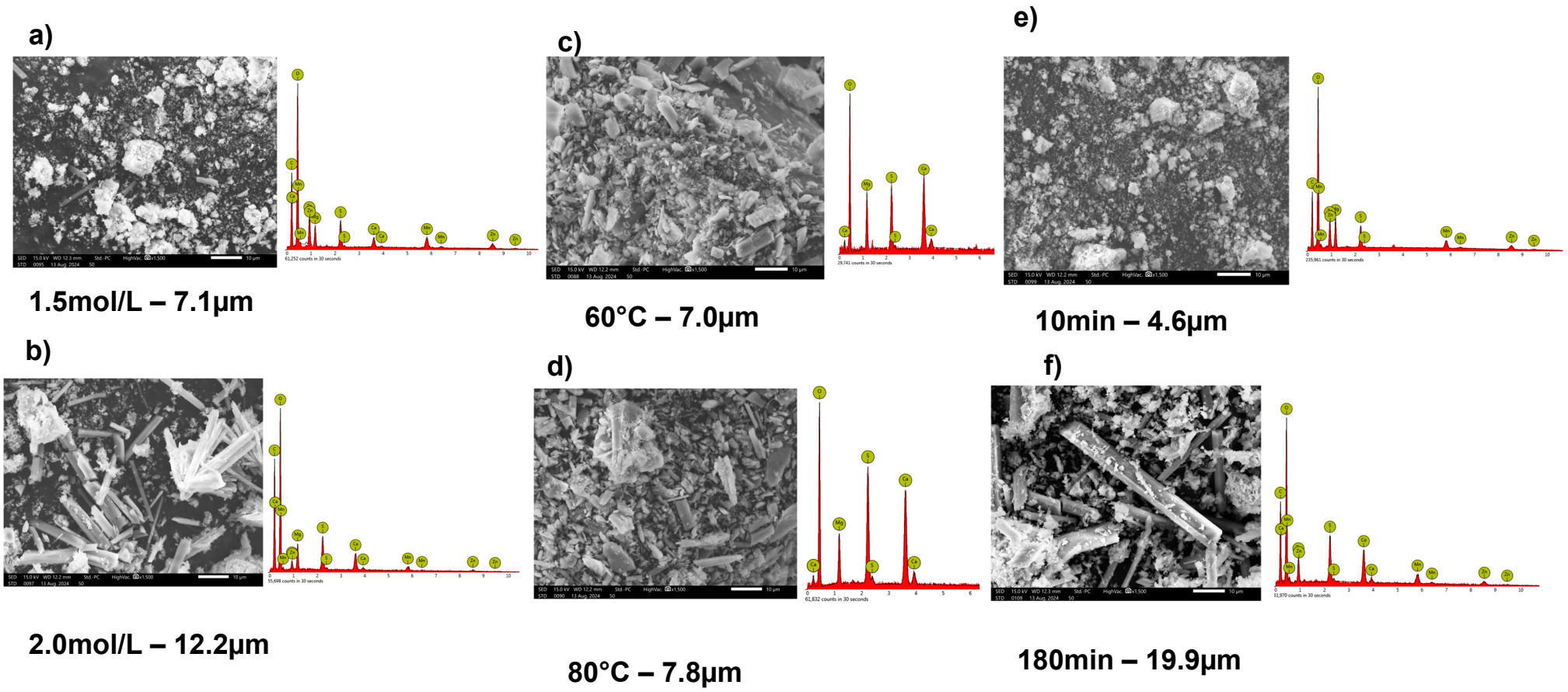

Figure 5. SEM images and EDS spectrum of precipitates formed in 1.5 mol/L (**a**), 2.0 mol/L (**b**), 60 °C (**c**), 80 °C (**d**), 10 min (**e**), and 180 min (**f**) experiments.

The $CaSO_4$ (2) seed exhibited a higher increase in the particle size (approximately 400% higher, Figure 6a and Table 5) in comparison with other seeds (S10, S20, and S30) due to the presence of other metals (e.g., Mn, Zn, and Mg) promoting a heterogeneous primary crystallization while the $CaSO_4$ (2) was only constituted by calcium sulfate [2]. A heterogenous primary crystallization has an increased nucleation rate, creating smallernucleus instead of promoting crystallization on the seed, which was the aim. The difference between the results achieved by $CaSO_4$ (1) (23.4 µm) and $CaSO_4$ (2) (40.8 µm) also demonstrated that the seed size influences the particle size.

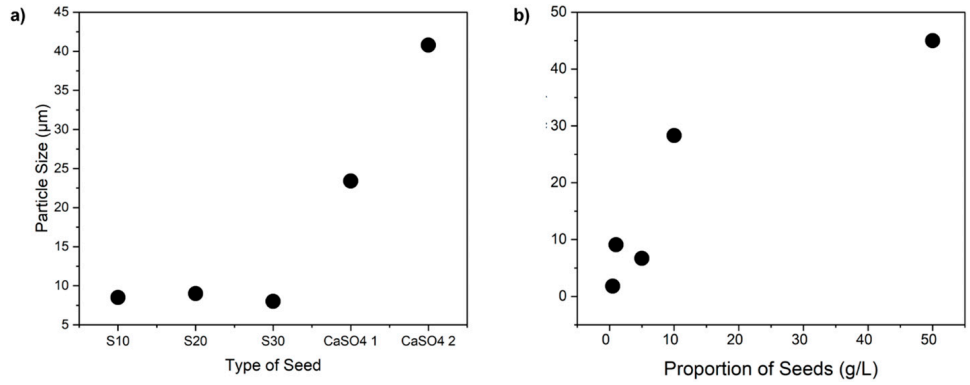

Figure 6. The effects of the type of seed (**a**) and the proportions of seeds (**b**) on the particle size.

The particle size distribution is proportional to the seeds added in the reaction (proportion of seeds) (Figure 6b), which can be explained by the secondary nucleation equation ($B_N = k_{n,s} N_i^j M_T^k \sigma^b$) which correlates with the secondary nucleation (B_N) and the mass of seeds added ($M^k{}_T$) [3]. Proportions of 10–100 g/L are expected to improve crystal growth when a system has slow kinetics. However, a proportion of 1.0 g/L improves the nucleation control, avoiding spontaneous nucleation but not necessarily affecting crystal growth. Crystals with a needle-like morphology demand more seeds than round crystals due to the surface area available for growth [3].

In seed crystallization, the ions in a supersaturated solution precipitate around the seed and make the crystal grow (Figure 7) instead of gathering in a cluster. The proportions of 0.5 g/L (Figure 8a), 5.0 g/L (Figure 8b), and 50.0 g/L (Figure 8c) demonstrated that the particle size increases with the increase in the proportion of seeds.

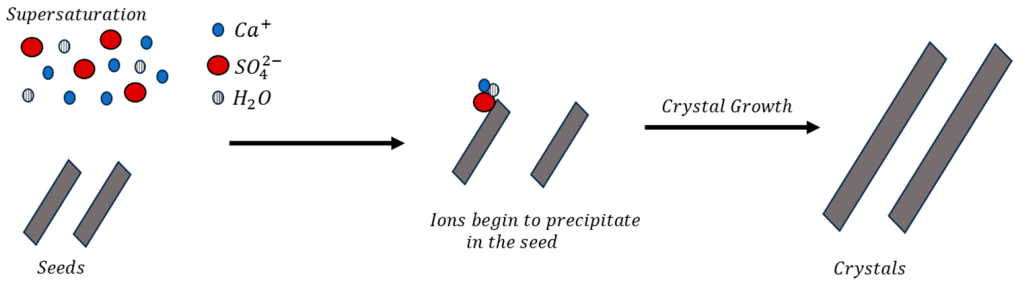

Figure 7. Diagram representing the seeding technique in nucleation.

3.4. Decantation Experiments

An experiment was conducted without the addition of any reagent for comparison, demonstrating an average speed of 50 mL/min (Table 6), to determine whether the increase in particle size observed in the precipitation tests and the addition of flocculants would impact the settling velocity.

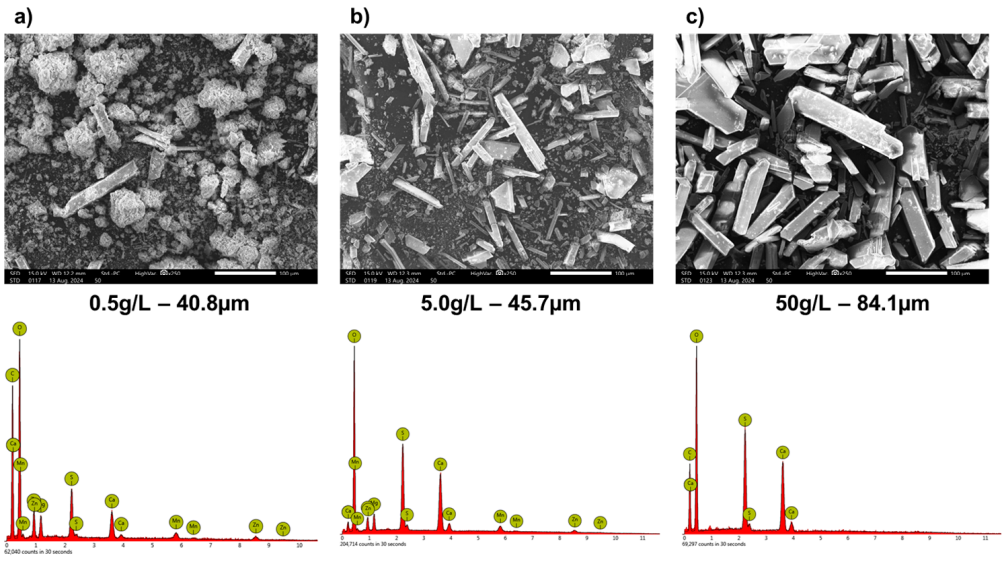

Figure 8. SEM images and EDS spectra of precipitates formed in 0.5 g/L (**a**), 5.0 g/L (**b**), and 50.0 g/L (**c**) seed proportions experiments.

Table 6. Average speed and growth % of the decantation experiments with different reagents.

Reagent	Average Speed	Increase in Average Speed %
-	50 mL/min	-
Seeds 10 g/L	110 mL/min	120%
F1 0.05% m/m	120 mL/min	140%
F2 0.05% m/m	140 mL/min	180%
F3 0.05% m/m	160 mL/min	220%
F4 0.01% m/m	166 mL/min	232%
Seeds 10 g/L and F4 0.01% m/m	177 mL/min	254%

The addition of seeds in a 10 g/L ratio caused a 700% increase in particle size and a 120% increase in the settling velocity that can be explained by Stokes' Law ($V = \frac{2}{9} \frac{(\rho_p - \rho_f)}{\mu} g \cdot R^2$), which correlates particle size (R) with the settling velocity (V) [24].

The use of coagulants and flocculants was also promising for increasing the average speed. F1 and F2 (Table 6) provided a 140% and 180% increase in speed, respectively, while F3 and F4 resulted in increases of 220% and 232%, respectively. The addition of seeds combined with F4 also demonstrated an increase of 254% in the decantation time in comparison to those without the use of coagulants, flocculants, or seeds.

The use of reagents helped increase the average speed due to their characteristics. Coagulants can neutralize the particle charges, clustering the particles, while flocculants have long carbon chains to aggregate particles [25]. F4 showed the best result due to its flocculant characteristic while the others are coagulants.

4. Conclusions

The aim of this study was to increase the settling velocity in the zinc mining tailing treatment by increasing the particle size of the precipitate. The effects of concentration, temperature, and time were evaluated, as well as the use of seeds, coagulants, and flocculants. When evaluating the parameters in experiments without seeds, increasing the concentration of the $Ca(OH)_2$ suspension from 1.0 mol/L to 2.0 mol/L resulted in a 70% increase in particle size, justified by the higher degree of supersaturation. An increase in

temperature did not favor particle growth, with the particle size at 80 °C being 40% smaller than at 25 °C, due to the solubility of $CaSO_4$ decreasing with rising temperature. Reaction time was a determining factor for particle growth, with a 300% increase observed from 10 min to 3 h, explained by the slow reaction kinetics and the Ostwald ripening. Regarding the use of seeds, it was found that the seed prepared according to the methodology of Chagwedera, Chivavava, and Lewis (2022) [12] resulted in particle sizes that were 400% larger than those obtained with recycled process seeds. As for the seed proportion, adding seeds in the range of 10–100 g/L led to a 700% increase in particle size. In the decantation experiments, it was possible to determine an increase in the decantation speed when using seeds (120% growth), the F4 flocculant in a 0.01% m/m rate (232% growth), and both (254% growth).

Author Contributions: Conceptualization, F.G.G.Z.; methodology, F.G.G.Z., A.B.B.J., M.M.S., D.C.R.E. and J.A.S.T.; investigation, F.G.G.Z.; resources, D.C.R.E. and J.A.S.T.; writing—original draft preparation, F.G.G.Z.; writing—review and editing, F.G.G.Z. and A.B.B.J.; supervision, M.M.S., D.C.R.E. and J.A.S.T. All authors have read and agreed to the published version of the manuscript.

Funding: This research was funded by FAPESP, grant number 2019/11866-5.

Data Availability Statement: The original contributions presented in this study are included in the article. Further inquiries can be directed to the corresponding author.

Acknowledgments: The authors thank the University of Sao Paulo for supporting this project and ABBJR would like to thank MIT Climate Grand Challenges.

Conflicts of Interest: The authors declare no conflicts of interest.

References

1. Lewis, A.; Seckler, M.; Kramer, H.; van Rosmalen, G. *Industrial Crystallization: Fundamentals and Applications*, 1st ed.; Cambridge University Press: Cambridge, UK, 2015; pp. 4–19, 71–128.
2. Mullin, J.W. *Crystallization*, 4th ed.; ButterWorth Heinemann: Oxford, UK, 2001; pp. 181–214.
3. He, Y.; Gao, Z.; Zhang, T.; Sun, J.; Ma, Y.; Tian, N.; Gong, J. Seeding Techniques and Optimization of Solution Crystallization Processes. *Org. Process Res. Dev.* **2020**, *20*, 1839–1849. [CrossRef]
4. Shang, Y.; Wang, Y.; Huang, J.; Shi, J.; Xu, L.; Li, K.; Jin, P.; Jin, X. A novel strategy for simultaneous removal of hardness, suspended solids and organics from fracturing wastewater: Efficiency, mechanism and application. *Sep. Purif. Technol.* **2025**, *366*, 132735. [CrossRef]
5. Reichl, C.; Schatz, M. *World Mining Data 2025*; International Organizing Committee for the World Mining Congress: Viena, Austria, 2025.
6. Talebi, M.; Rezaei, A.; Rafiei, Y. Application of sodium carbonate and sodium sulfate for removal of lithium and strontium from oilfield produced water. *Sci. Rep.* **2025**, *15*, 18895. [CrossRef] [PubMed]
7. Huang, J.; Shang, Y.; Xu, Y.; Shen, L.; Wang, Y.; Liu, Y.; Zhang, G.; Mei, A.; Liu, H.; Jin, P. Study on the nucleation crystallization pelleting process for manganese ion recovery from hydrometallurgical tailings water. *Front. Environ. Sci. Eng.* **2025**, *19*, 98. [CrossRef]
8. Yang, J.; Chen, L.; Yang, L.; Jiang, X.; Deng, L.; Tang, X.; Wang, W. Organic matter removal mitigates crystallization inhibition to enhance co-recovery of potassium and phosphorus from wastewater. *Enrivon. Res.* **2025**, *279*, 121758. [CrossRef] [PubMed]
9. Jorge, N.; Amor, C.; Teixeira, A.R.; Marchão, L.; Lucas, M.S.; Peres, J.A. Combination of Coagulation-Flocculation-Decantation with Sulfate Radicals for Agro-Industrial Wastewater Treatment. *Eng. Proc.* **2022**, *19*, 19.
10. Alimi, F.; Elfil, H.; Gadri, A. Kinetics of the precipitation of calcium sulfate dihydrate in a desalination unit. *Desalination* **2003**, *158*, 9–16. [CrossRef]
11. Magomedzapir, S.; Ali, K.; Artigat, B.; Zarima, G.; Tamila, M. The disinfecting properties of Penox-1 solutions for sanitation of objects of veterinary supervision. *E3S Web Conf.* **2020**, *175*, 03012.
12. Chagwedera, T.M.; Chivavava, J.; Lewis, A.E. Gypsum Seeding to Prevent Scaling. *Crystals* **2022**, *12*, 342. [CrossRef]
13. Brough, D.; Jouhara, H. The aluminium industry: A review on state-of-the-art technologies, environmental impacts and possibilities for waste heat recovery. *Int. J. Thermofluids* **2020**, *1–2*, 100007. [CrossRef]
14. Chaves, A.P. *Teoria e Prática do Tratamento de Minérios: Desaguamento, Espessamento e Filtragem*, 3rd ed.; Signus: Rio de Janeiro, Brasil, 2010; pp. 50–85.

15. Mondillo, N.; Accardo, M.; Boni, M.; Boyce, A.; Herrington, R.; Rumsey, M.; Wilkinson, C. New insights into the genesis of willemite (Zn_2SiO_4) from zinc nonsulfide deposits, through trace elements and oxygen isotope geochemistry. *Ore Geol. Rev.* **2020**, *118*, 103307. [CrossRef]
16. Xu, H.; Qian, Y.; Zhou, Q.; Wei, C.; Wang, Q.; Zhao, W.; Zhu, B.; Tong, F.; Ren, F.; Zhang, M.; et al. Leaching of Willemite Concentrate in Sulfuric Acid Solution at High Temperature. *Sustainability* **2023**, *15*, 161. [CrossRef]
17. Olivo, G.R.; Monteiro, L.V.; Baia, F.; Slezak, P.; Carvalho, I.; Fernandes, N.A.; Oliveira, G.D.; Botura Neto, B.; McGladrey, A.; Silva, A.M.; et al. The Proterozoic Vazante hypogene zinc silicate district, Minas Gerais, Brazil: A review of the ore system applied to mineral exploration. *Minerals* **2018**, *8*, 22. [CrossRef]
18. Abdel-Aal, E.A.; Rashad, M.M.; El-Shall, H. Crystallization of calcium sulfate dihydrate at different supersaturation ratios and different free sulfate concentrations. *Cryst. Res. Technol.* **2004**, *39*, 313–321. [CrossRef]
19. Kumar, S.; Naiya, T.K.; Kumar, T. Developments in oilfield scale handling towards green technology-A review. *J. Pet. Sci. Eng.* **2018**, *169*, 428–444. [CrossRef]
20. Bahrig, L.; Hickey, S.G.; Eychmüller, A. Mesocrystalline materials and the involvement of oriented attachment—A review. *CrystEngComm* **2014**, *16*, 9408–9424. [CrossRef]
21. Luo, K.; Li, C.; Xiang, L.; Li, H.; Ning, P. Influence of temperature and solution composition on the formation of calcium sulfates. *Particuology* **2010**, *8*, 240–244. [CrossRef]
22. Lochhead, R.Y. Basic Physical Sciences for the Formulation of Cosmetic Products. In *Cosmetic Science and Technology: Theoretical Principles and Applications*, 1st ed.; Elsevier Inc.: Amsterdam, The Netherlands, 2017; pp. 39–76.
23. Sugimoto, T. Recrystallization. In *Monodispersed Particles*, 2nd ed.; Elsevier: Amsterdam, The Netherlands, 2019; pp. 167–179.
24. Moran, S. Fluid mechanics. In *An Applied Guide to Water and Effluent Treatment Plant Design*, 1st ed.; Elsevier: Amsterdam, The Netherlands, 2018; pp. 53–58.
25. Bratby, J. *Coagulation and Flocculation in Water and Wastewater Treatment*, 3rd ed.; IWA Publishing: London, UK, 2016.

Disclaimer/Publisher's Note: The statements, opinions and data contained in all publications are solely those of the individual author(s) and contributor(s) and not of MDPI and/or the editor(s). MDPI and/or the editor(s) disclaim responsibility for any injury to people or property resulting from any ideas, methods, instructions or products referred to in the content.